Electronic Supporting Information

Light Atom Influenced Room Temperature Phosphorescence in Functionalized Benzophenones: Experimental and Theoretical Correlations

Anila M. Menon[a], Debranjan Hati[b], Ankita Kumari[c], Swadhin Garain[b], Durgesh Pandey[c], Rahul Shukla[e], Dibyajyoti Ghosh[c,d], Deepak Chopra*[a]*

Contents

Materials and Methods

Materials

All the substituted benzophenones used in this study were procured from Sigma-Aldrich and Alfa Aesar and were used without further purification.

Experimental Methods

- ***Crystallization***

All the substituted benzophenones (**Scheme 1**) were crystallized under diverse solvent conditions and at two temperature regimes - (room temperature (22-24 °C) and low temperature (4 °C)). A comprehensive approach to polymorphism was explored and structurally characterized via SCXRD.

- ***Single Crystal X-ray Diffraction (SCXRD)***

The substituted benzophenones were characterized using the single-crystal X-ray diffraction technique. The SCXRD data were collected on a *Bruker D8 Venture PHOTON 100 CMOS* instrument, equipped with a four-circle Kappa diffractometer, a collimated molybdenum (MoKα = 0.71073 Å) source, and a *PHOTON III C14* detector. Data reduction was carried out using the Bruker *SAINT,* and numerical absorption correction was applied via Bruker *SADABS-2014/5*[1]. Refinement was performed using the full matrix least squares method in *SHELXL-2018*[2], integrated within the *Olex2* programme suite. All the geometric calculations were performed from *PARST*[3]. The crystal packing analysis for all the obtained compounds was explored using *Mercury 4.2.0*[4]. Further, the thermal ellipsoidal plots were generated via *Mercury 4.2.0*.

- ***Powder X-ray Diffraction (PXRD)***

The powder X-ray diffraction data for all crystalline solids were collected on a *PANalytical Empyrean* diffractometer with a copper (CuKα = 1.5406 Å) source and *PIXcel3D* detector. Measurements were performed at room temperature with a step size of 0.013° and a 2θ scan range of 5° to 60° (**Fig. S1**).

- ***Thermal Techniques***

The thermal stability of all solid samples was examined using differential scanning calorimetry (DSC)[5]. DSC quantitatively analyzes various phase changes in the crystal, including melting point and enthalpy changes, as a function of temperature. DSC experiments were performed on *Perkin Elmer DSC 6000* instrument, at a scan rate of 5 °C/min (**Fig. S2**).

- ***Conformational Analysis***

The gas phase optimization of the crystal geometry was performed using B3LYP/6-31G (d,p) level basis set in *Gaussian09* software[6]. The relative potential energy scan was performed by rotating the torsions from 0° to 360° **(Scheme 1)**.

- ***Fingerprint plots and d_{norm} plots***

These plots were generated from *Crystal Explorer21.5* software[7], wherein the distances from the surface to the nearest atomic nuclei-inside (d_i) and outside (d_o) the surface-were calculated to reveal the nature of intermolecular interactions. These are then translated into 2D fingerprint plots[8-9], offering a visual representation of the various interaction contributions made by the molecule, due to the presence of the neighbouring molecules.

The normalized contact distances (d_{norm}) between atoms highlight regions of close contact, typically corresponding to significant intermolecular interactions. On the surface, red spots represent contacts shorter than the sum of van der Waals radii, indicating strong interactions; white areas correspond to contacts close to van der Waals radii, suggesting neutral interactions, and blue regions denote longer contacts, usually associated with weak interactions.

- ***Energy frameworks from Crystal Explorer and PIXEL Calculations***

Theoretical calculations were conducted using *Crystal Explorer 21.5*, with wavefunction generated via *TONTO* program using B3LYP/6-31G (d,p) level. To explore intermolecular interactions[10], energy frameworks were constructed by utilizing a cluster of molecules of 3.8 Å radius. The strength of interactions was then visualized by the thickness of cylindrical tubes. Further, the lattice energy for all the benzophenone derivatives was calculated by utilizing a molecular cluster of 20 Å radius.

The precise intermolecular interaction energies for the molecular pairs are computed using *PIXELC* module of the CLP computer program[11-12], which incorporates neutron-normalized values for the hydrogen atoms in the computation. The total interaction energy is expressed in

terms of coulombic, polarization, dispersion and repulsion components[13]. The interaction energies below a specific threshold energy value (-4 kJ/mol) are excluded from further analysis. Additionally, the percentage contributions of dispersion and electrostatic energy to the overall stabilization energy are determined.

- ***Instrumentation for investigation of RTP***

Spectroscopic Measurements: The excitation and emission spectra were recorded on FLS1000 spectrometer, Edinburgh Instruments.

Lifetime and quantum yield measurements: phosphorescence lifetime ($\lambda_{exc.}$ = 360 nm), gated emission, and time-resolved emission were measured on FLS1000 spectrometer, Edinburgh Instruments equipped with a micro flash-lamp (μF2) set-up. Quantum yields were measured using an integrating sphere in the same instrument.

- ***Quantum Theory of Atoms in Molecules (QTAIM) analysis***

The topological properties of the electon density distribution in all molecular motifs considered here were analysed by QTAIM approach[14]. This was computed using B3LYP/6-31G (d,p) level of theory in AIMALL programme suite[15]. The bonding nature of non-covalent interactions were determined by the presence of (3, -1) bond critical points and bond paths between interacting atoms. Further, the ratio of potential energy to the kinetic energy densities ($|V|$/G) determines the nature of interactions to be closed-shell or shared-shell/covalent interactions.

- ***Computational Details***

Density functional theory (DFT)-based simulations were carried out using the QUICKSTEP module in the CP2K package to investigate the static and electronic properties of RTP under various substitutions[16]. These simulations employed a combination of Gaussian and plane-wave (GPW) approach, with an energy cut-off set at 300 Ry. A double-ζ polarized MOLOPT short-range basis set was used, along with analytical dual-space Goedecker-Teter-Hutter pseudopotential[17]. Wherein, the generalized gradient approximation (GGA) by Perdew-Burke-Ernzerhof (PBE) as the exchange-correlation functional for geometry was utilized[18]. The geometry optimization was performed using the conjugate gradient method until the force on each atom dropped below 0.01 eV $Å^{-1}$. To accurately evaluate the electronic properties, a highly precise range-separated hybrid exchange-correlation functional (HFX) was further employed[19]. In which ADMM basis sets were used for HFX calculations in CP2K. Specifically,

auxiliary MOLTOP-ADMM basis functions were applied, with FIT9 employed for oxygen and FIT3 for carbon, hydrogen and fluorine[20-21].

- ***Theoretical Calculations***

Time-dependent density functional theory (TD-DFT) calculations were performed by optimizing the crystal structure in the *Gaussian09* software package[22], by employing the B3LYP functional and the 6-31G(d,p) basis set. This approach enables the characterization of excited electronic states, including singlets and triplets, through the derivation of electron density based on self-consistent field (SCF) theory[23]. Additionally, the energy levels of the HOMO-LUMO orbitals were investigated.

Table S1. Details of Crystallization experiments.

Sample code	Solvent Used	Morphology	Result
2F4′FBZP	Acetonitrile	-	- : No crystals Plate: 2F4′FBZP
	Toluene*	Plate	
	Methanol	-	
	Ethanol	-	
	Benzene	-	
	Nitromethane	-	
3F3′FBZP	Acetonitrile*	Plate	Plate: 3F3′FBZP
	Toluene	Aggregate	
	Methanol	Plate	
	Ethanol	Plate	
	Benzene	Aggregate	
	Nitromethane	Plate	
4FBZP	Acetonitrile	Plate	Plate: 4FBZP
	Toluene	Aggregate	
	Methanol	Plate	
	Ethanol	Plate	
	Benzene	Aggregate	
	Nitromethane	Plate	
	Dioxane*	Plate	
4MBZP_I & 4MBZP_II	Acetonitrile	Aggregate	Block: 4MBZP_I Plate: 4MBZP_II
	Toluene	Aggregate	
	Methanol	Block	
	Ethanol*	Block & Plate	
	Benzene	Aggregate	
	Nitromethane	Aggregate	

*** Indicates that the SCXRD data was collected on the crystals obtained from these solvent systems.**

Table S2. Crystallographic data.

Sample name	2F4′FBZP	3F3′FBZP	4FBZP	4MBZP_I	4MBZP_II
Crystal System	Orthorhombic	Monoclinic	Monoclinic	Triclinic	Monoclinic
Formula	$C_{13}H_8F_2O$	$C_{13}H_8F_2O$	$C_{13}H_9FO$	$C_{14}H_{12}O_2$	$C_{14}H_{12}O_2$
Formula weight	218.19	218.19	200.20	212.24	212.24
CCDC no.	**2254727**	**2254723**	**2475519**	**2475520**	**2254724**
Space Group	$P2_12_12_1$	$C2/c$	$P2_1/n$	P-1	Cc
Temperature(K)	100.00	100.00	100.00	109.00	101.00
***a* (Å)**	8.9425(16)	23.019(4)	6.0877(3)	9.1733(3)	23.943(5)
***b*(Å)**	9.8311(13)	6.1377(7)	21.9520(15)	9.4825(3)	7.3692(11)
***c*(Å)**	11.522(2)	7.1577(11)	7.3093(5)	13.8732(10)	6.1423(11)
***α* (°)**	90	90	90	87.9240(10)	90
***β* (°)**	90	99.771(6)	90.168(2)	71.201(2)	98.999(8)
***γ* (°)**	90	90	90	70.4990(10)	90
Volume [V(Å^3)]	1012.9(3)	996.6(2)	976.79(11)	1073.42(6)	1070.4(3)
Density (g/cm^3)	1.431	1.454	1.361	1.313	1.317
Z', Z	1, 4	0.5, 4	1, 4	1, 4	1, 4
Size of crystal (mm^3)	0.736 × 0.182 × 0.14	0.286 × 0.137 × 0.116	0.361 × 0.208 × 0.09	0.260 × 0.188 × 0.181	0.227 × 0.159 × 0.069
μ/mm^{-1}	0.115	0.116	0.098	0.087	0.087
***F* (000)**	448.0	448.0	416.0	448.0	448.0
θ $_{min,max}$	2.724, 30.047	3.439, 30.034	2.937, 30.028	2.286, 30.030	2.895, 30.110
h $_{min,max}$	-12, 12	-32, 32	-8, 8	-12, 12	-33, 33
k $_{min,max}$	-13, 13	-8, 8	-30, 30	-13, 13	-10, 10
l $_{min,max}$	-16, 16	-9, 10	-10, 10	-19, 19	-8, 8
No. of reflections	30579	12661	62754	95716	15606
No. of unique/ observed reflections	2975, 2481	1450, 903	2852, 2509	6265, 5487	3148, 1937
No. of parameters	145	74	145	291	146
R $_{all}$, R $_{obs}$	0.0535, 0.0437	0.0825, 0.0475	0.0913, 0.0848	0.0475, 0.0414	0.1097, 0.0663
wR2 $_{all}$, wR2 $_{obs}$	0.1114, 0.1067	0.1278, 0.1175	0.2573, 0.2537	0.1171, 0.1107	0.1718, 0.1562
$\Delta\rho_{max,min}$(eÅ^{-3})	0.30, -0.36	0.28, -0.26	0.47, -0.36	0.42, -0.22	0.37, -0.38
G.o.F	1.063	1.030	1.157	1.026	0.972

Table S3(a). Intermolecular interactions along with interaction energies (in kJ mol^{-1}). The neutron normalised values are mentioned here.

Motifs	Symmetry code	Centroid−Centroid distance (Å)	E_{Coul}	E_{Pol}	E_{Disp}	E_{Rep}	E_{Tot} (PIXEL) kJ mol^{-1}	E_{Tot} (Crystal Explorer) kJ mol^{-1}	Involved Interactions Geometry (Å/°) D(D···A), d(H···A), ∠D−H···A
2F4′FBZP (Z′=1)									
I	-x+1, +y+1/2, -z+1/2+1	6.411	-6.9	-3.3	-19.6	14.0	**-15.8**	**-17.3**	C10-H10···O1 3.497(3), 2.56, 145 C10-H10···C13 3.552(2), 2.77, 140 C7-H7···F2 3.690(2), 2.66, 159
II	-x+1/2+1, -y+1, +z-1/2	7.513	-6.2	-2.7	-18.0	12.7	**-14.2**	**-15.8**	C5-H5···F1 3.278(3), 2.38, 140
III	-x+1/2+1, -y, +z+1/2	8.230	-6.8	-3.1	-12.5	8.5	**-14.0**	**-14.3**	C12-H12···O1 3.494(2), 2.59, 141
IV	x, +y, +z-1	11.522	-2.9	-0.9	-7.8	4.2	**-7.4**	**-6.9**	C5-H5···F2 3.312(2), 2.48, 133
V	x+1/2, -y+1/2, -z+2	10.178	-2.5	-0.9	-6.4	4.9	**-4.8**	**-5.7**	C12-H12···F2 3.114(3), 2.52, 114
3F3′BZP (Z′=1)									
I	-x+1, +y-1, -z+1/2	6.138	-11.2	-3.9	-22.1	15.3	**-22.0**	**-22.5**	C7-H7···O1 3.308(2), 2.60, 123
II	-x+1, -y, -z	5.444	-6.9	-5.3	-32.8	24.7	**-20.2**	**-22.7**	C7-H7···H7-C7 2.29, 145, 145
III	-x+1/2+1, -y+1/2, -z+1	11.505	-4.5	-0.8	-6.6	3.4	**-8.6**	**-9.4**	C5-H5···F1 3.377(2), 2.67, 123
IV	-x+1/2+1, +y-1/2, -z+1/2	11.912	-1.9	-0.9	-4.4	3.1	**-4.1**	**-4.1**	C5-H5···F1 3.425(2), 2.46, 148
4FBZP (Z′=1) (Reported data) [24]									
I	x+1,+y,+z	6.088	-10.3	-4.6	-21.5	14.4	**-22.0**	**-22.2**	C7-H7···O1 3.256(3), 2.60, 119 C13-H13···O1 3.289(3), 2.62, 120
II	x+1/2,-y+1/2+1,+z+1/2	4.811	-7.1	-4.7	-36.1	25.8	**-22.0**	**-26.2**	C6-H6···C13 3.704(3), 2.95, 137 C6-H6···C12 3.909(3), 3.00, 160 C3-H3···C9 3.929(3), 3.06, 158 C3-H3···C10 3.803(3), 3.07, 135
III	x-1/2,-y+1/2+1,+z+1/2	4.825	-6.2	-4.2	-35.8	24.6	**-21.7**	**-25.4**	C9-H9···C4 3.676(2), 2.93, 137 C9-H9···C3 3.924(3), 3.03, 158 C12-H12···C7 3.809(3), 3.08, 158 C12-H12···C6 3.909(3), 3.06, 135
IV	-x+1,-y+2,-z+1	10.344	-4.5	-1.7	-11.7	9.4	**-8.5**	**-7.6**	C4-H4···F1 3.426(4), 2.48, 146
V	-x+1,-y+1,-z+1	11.868	-1.9	-0.5	-7.1	2.4	**-7.1**	**-6.3**	C10-H10···F1A 3.430(5), 2.81, 117
VI	-x+1/2+1,+y-1/2,-z+1/2+1	11.444	-1.0	-0.4	-4.8	1.7	**-4.5**	**-4.4**	C10-H10···F1 3.363(4), 2.70, 120
VII	-x+2,-y+2,-z+1	12.644	1.3	-0.3	-3.4	0.8	**-1.6**	**-2.0**	C5-H5···F1 3.531(4), 2.61, 143 F1···F1

									2.409(5), 148, 148
VIII	-x+2,-y+1,-z+1	11.226	-0.9	-0.4	-4.9	15.4	**9.2**	**1.8**	C11-H11···F1A 3.362(5), 2.46, 141 F1A···F1A 2.260 (6), 141, 141
4MBZP_I (Z′=1) (Reported data) [25]									
I (b…b)	-x+2,-y+1,-z+1	7.781	-19.1	-4.8	-19.3	13.2	**-30.1**	**-31.2**	C28-H28A···O3 3.535(1), 2.58, 147
II (a…a)	-x+2,-y,-z+1	7.494	-21.0	-5.8	-22.3	20.4	**-28.7**	**-31.7**	C14-H14B···O1 3.449(1), 2.42, 158
III (a…b)	-x+1,-y+1,-z+1	5.504	-8.6	-4.9	-40.7	28.2	**-26.0**	**-28.7**	C27-H27···O2 3.264(1), 2.77, 108 C6-H6···C17 3.702(1), 2.84, 152
IV (a…b)	-x+2,-y+1,-z+1	7.256	-15.8	-6.1	-33.0	29.7	**-25.2**	**-30.1**	C3-H3···O4 3.522(1), 2.65, 137 C14-H14A···O3 3.384(2), 2.59, 130 C4-H4···C20 3.622(1), 2.88, 136 C14-H14A···C16 3.697(1), 2.87, 143 C13-H13···C15 3.603(2), 2.87, 135
V (a…b)	x, y+1,+z	4.838	-4.7	-3.9	-34.5	22.4	**-20.7**	**-23.4**	C20-H20···C6 3.782(1), 2.88, 160 C20-H20···C7 3.626(1), 2.90, 135
VI (a…a)	-x+2,-y,-z	9.489	-11.8	-4.1	-16.6	12.5	**-20.0**	**-19.2**	C10-H10···O1 3.536(1), 2.66, 138
VII (b…b)	-x+2,-y+1,-z	9.430	-8.6	-3.4	-14.4	9.3	**-17.1**	**-17.0**	C24-H24···O3 3.518(1), 2.69, 133
4MBZP_II (Form II) Z′=1									
I	x, -y+1, +z-1/2	4.726	-6.8	-6.7	-46.3	33.5	**-26.4**	**-30.4**	C14-H14C···C5 3.619(5), 2.89, 132
II	x, -y, +z+1/2	4.868	-8.3	-5.5	-39.7	29.5	**-24.0**	**-28.4**	C3-H3···C4 3.638(5), 2.87, 138
III	x, +y, +z-1	6.142	-9.0	-5.2	-23.8	13.9	**-24.0**	**-23.0**	C7-H7···O1 3.314(5), 2.67, 118 C13-H13···O1 3.357(5), 2.71, 118
IV	x-1/2, -y+1/2, +z-1/2	11.885	-5.6	-2.3	-10.3	10.4	**-7.7**	**-6.7**	C11-H11···O2 3.408(5), 2.34, 170

.

Table S3(b). Comparison of results from *PIXEL* with LMO-EDA scheme.

Dimer	E_{elec}	E_{pol}	E_{disp}	$E_{ex\text{-}rep}$	E_{total}	Methods
2F4′FBZP						
I	-10.5	-7.1	-28.7	31.3	-15.0	LMO-EDA
	-6.9	-3.3	-19.6	14.0	-15.8	PIXEL
	-6.5	-0.9	-18.9	9.0	-17.3	CE
II	-7.5	-4.6	-24.1	22.3	-13.8	LMO-EDA
	-6.2	-2.7	-18.0	12.7	-14.2	PIXEL
	-5.6	-0.7	-17.7	8.2	-15.8	CE
III	-8.3	-4.4	-12.1	12.6	-11.5	LMO-EDA
	-6.8	-3.1	-12.5	8.5	-14.0	PIXEL

	-7.4	-1.6	-10.9	5.6	-14.3	CE
IV	-3.8	-2.2	-8.0	8.3	-5.7	LMO-EDA
	-2.9	-0.9	-7.8	4.2	-7.4	PIXEL
	-2.7	-0.3	-6.9	3.1	-6.9	CE
V	-4.0	-2.3	-8.1	10.4	-4.0	LMO-EDA
	-2.5	-0.9	-6.4	4.9	-4.8	PIXEL
	-2.2	-0.3	-6.5	3.3	-5.7	CE
3F3′FBZP						
I	-17.0	-7.2	-34.9	38.0	-21.0	LMO-EDA
	-11.2	-3.9	-22.1	15.3	-22.0	PIXEL
	-11.5	-2.1	-19.3	10.4	-22.5	CE
II	-12.0	-8.5	-54.3	52.5	-22.4	LMO-EDA
	-6.9	-5.3	-32.8	24.7	-20.2	PIXEL
	-5.9	-1.3	-30.6	15.1	-22.7	CE
III	-7.7	-2.5	-9.9	11.6	-8.5	LMO-EDA
	-4.5	-0.8	-6.6	3.4	-8.6	PIXEL
	-4.8	-0.4	-7.0	2.7	-9.4	CE
IV	-2.9	-2.4	-5.0	7.5	-2.8	LMO-EDA
	-1.9	-0.9	-4.4	3.1	-4.1	PIXEL
	-1.7	-0.3	-4.4	2.3	-4.1	CE

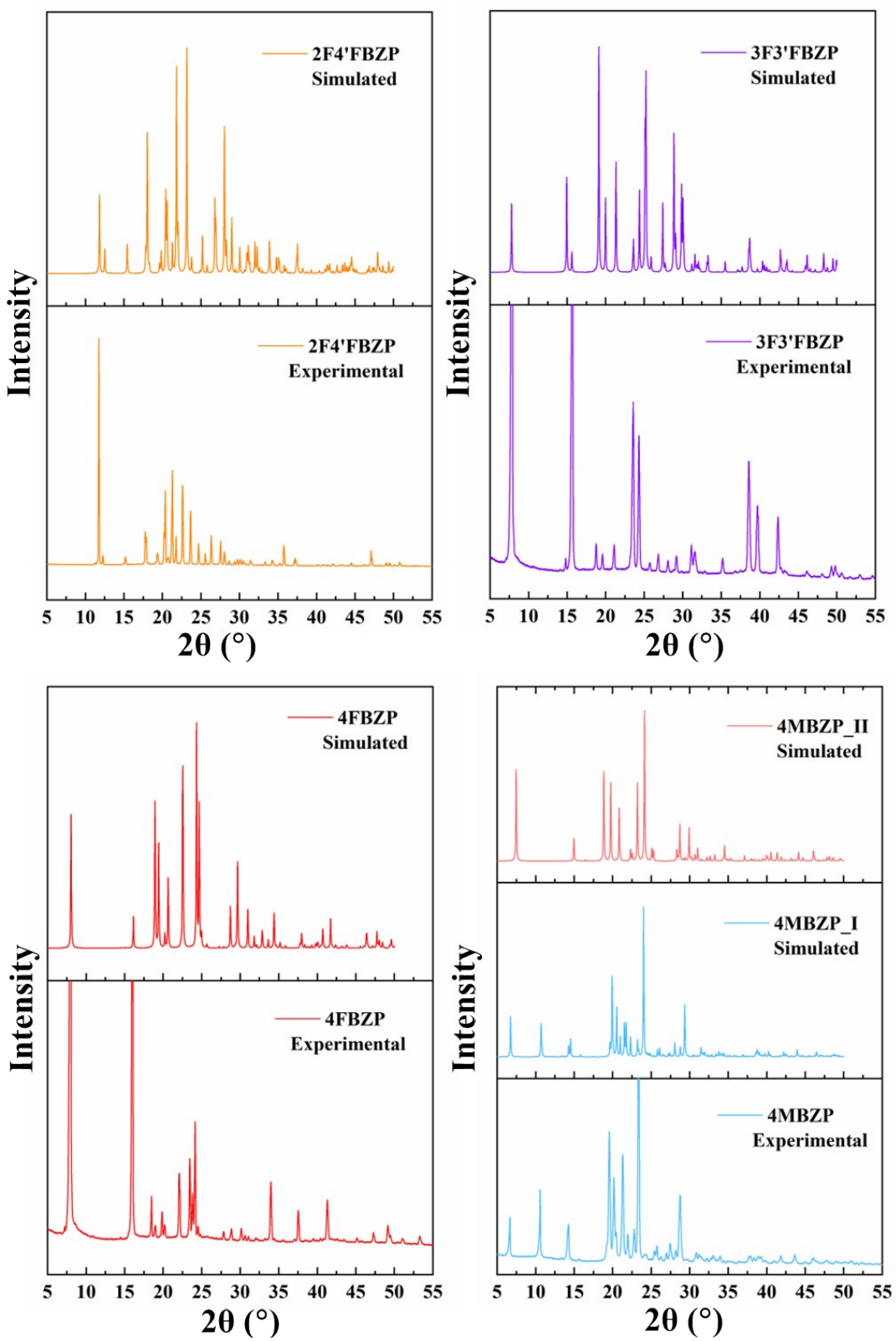

Fig. S1 Comparison of simulated and experimental powder patterns in substituted benzophenones.

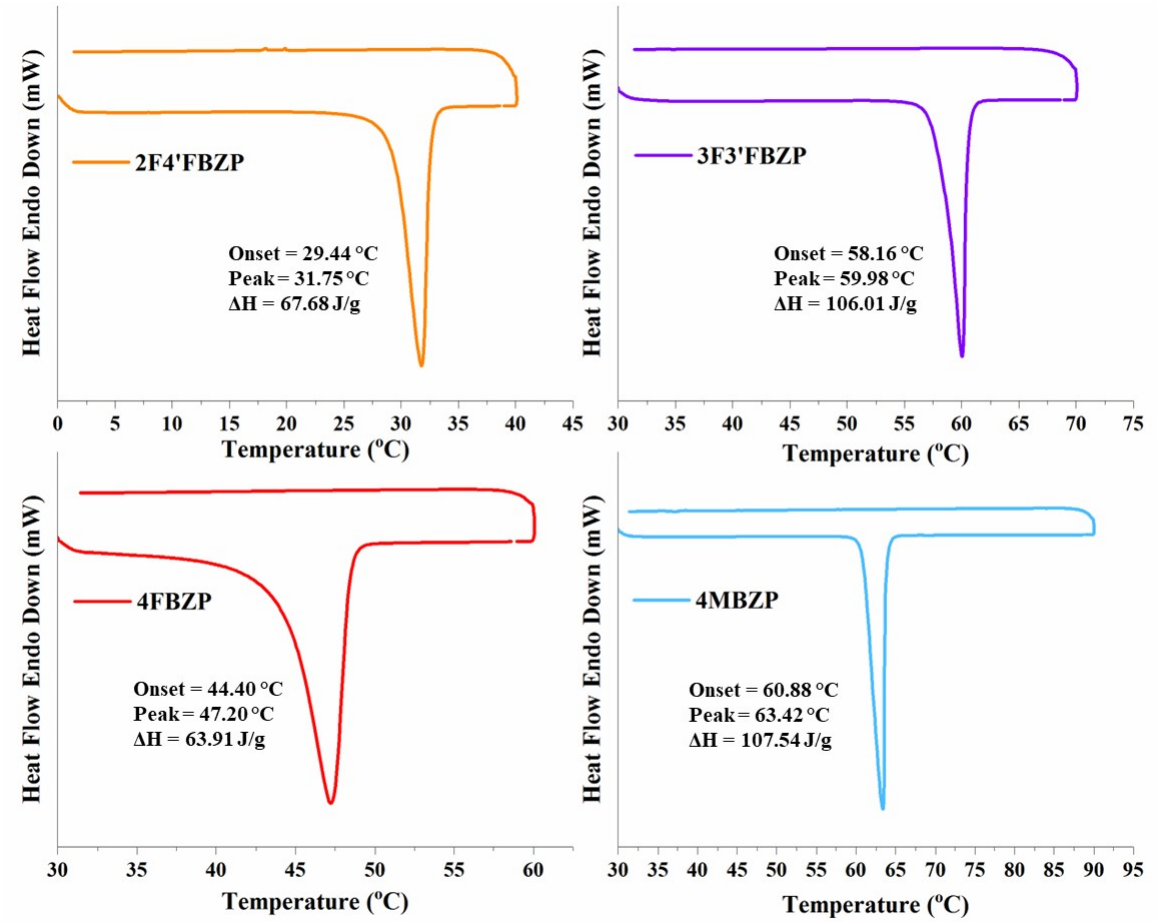

Fig. S2 DSC traces of functionalized benzophenones.

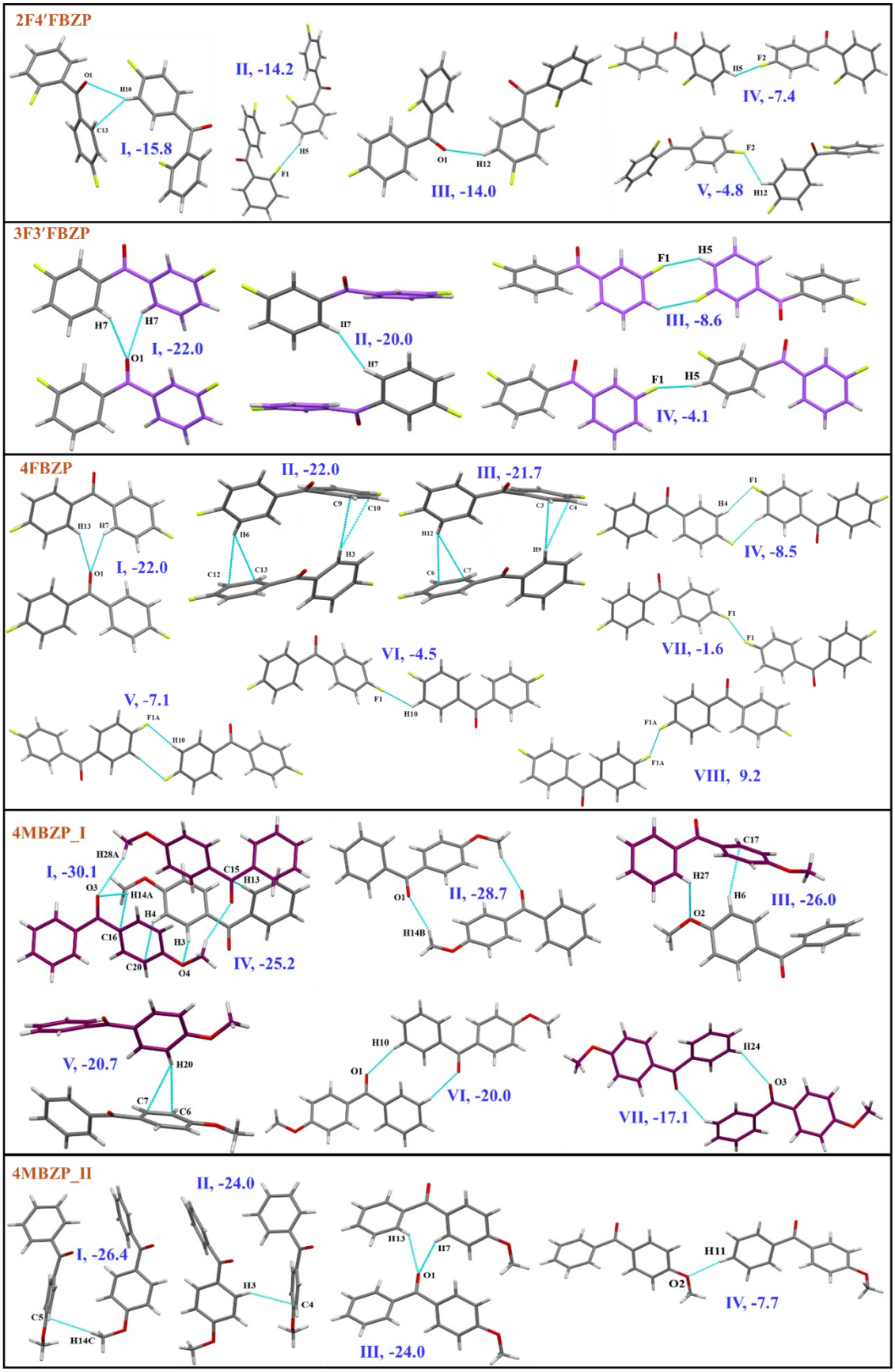

Fig. S3 Molecular pairs depicting the interaction energies in (kJ/mol) in blue *via PIXEL* method.

Hirshfeld analysis: d_{norm} plots and Fingerprint plots

The distances d_e and d_i mapped on the Hirshfeld surface provide intermolecular close contacts within the crystal, where d_e and d_i correspond to the distances from a point on the generated surface to the nearest external and internal atoms, respectively. To accurately determine close contacts, the normalized distance d_{norm} was utilized. A negative d_{norm} (shown in red) signifies contacts shorter than the van der Waals separation, while a positive d_{norm} (shown in blue) indicates larger contacts. For instance, in 4MBZP_II, the methoxy oxygen participates in C-H···O interactions, while in 4MBZP_I, this interaction is primarily mediated by the carbonyl oxygen. These distinct types of interactions are evident from the d_{norm} plots, as shown in **Figure S4**.

The Hirshfeld surface for all the molecules was first constructed to generate 2D fingerprint plots with d_e and d_i mapped onto them. Among the benzophenone derivatives, the reciprocal H···H contacts were found to be significantly pronounced. In 3F3′FBZP, the sharp characteristic spike diagonally aligned in the plot confirms the presence of H···H contact and well corresponds to the observed crystal packing pattern. Additionally, the presence of characteristic "wings" in fingerprint plots imply C-H···π contacts. The reciprocal contact values for C-H···π contacts were prominent when compared to other contacts, as also evident from crystal packing. Moreover, the minor contribution due to the presence of weak F···F halogen contact was noticed in 2F4′FBZP (1.9%), 3F3′FBZP (2.8%) and 4FBZP (2.3%). Furthermore, dispersive C-H···F interactions were prominently observed across all the benzophenone derivatives, including 2F4′FBZP, 3F3′FBZP, and 4FBZP (**Figure S5**).

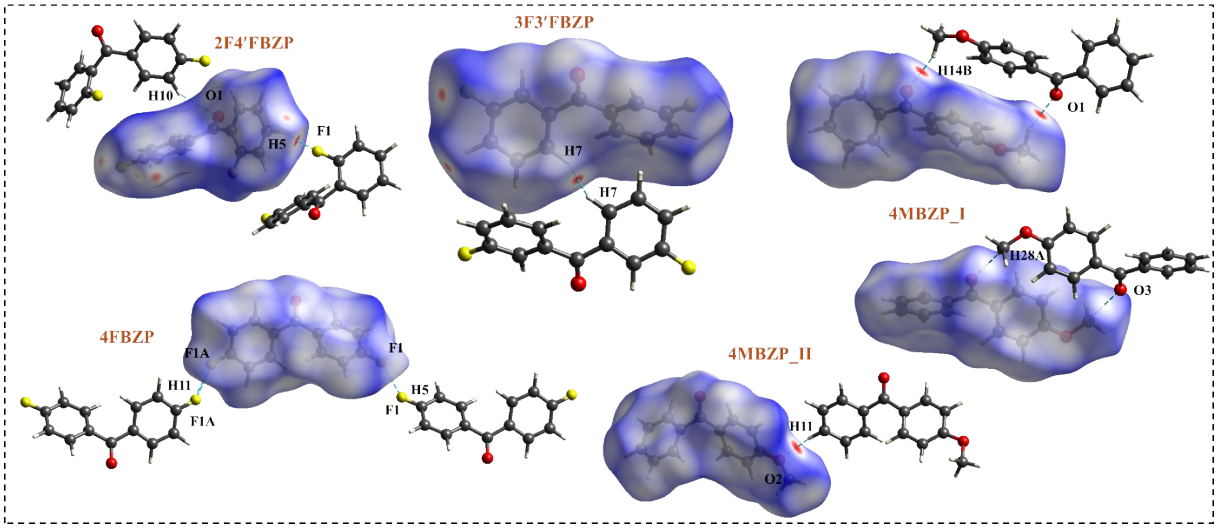

Fig. S4 d_{norm} plots highlighting the relevant motifs of benzophenone derivatives.

Table S4. Distribution of Intermolecular Interaction Energies as obtained from *CrystalExplorer.*

These were calculated utilizing the B3LYP/6-31G (d,p) functional basis set.

Information

Crystal | Atoms | Surface | Energies

2F4′FBZP

Interaction Energies (kJ/mol)
R is the distance between molecular centroids (mean atomic position) in Å.

Total energies, only reported for two benchmarked energy models, are the sum of the four energy components, scaled appropriately (see the scale factor table below)

	N	Symop	R	Electron Density	E_ele	E_pol	E_dis	E_rep	E_tot
	2	-x, y+1/2, -z+1/2	6.41	B3LYP/6-31G(d,p)	-6.1	-1.2	-21.8	14.6	-17.3
	2	-x+1/2, -y, z+1/2	8.23	B3LYP/6-31G(d,p)	-7.0	-2.2	-12.5	9.0	-14.3
	2	-x, y+1/2, -z+1/2	9.82	B3LYP/6-31G(d,p)	-0.3	-0.5	-9.0	5.4	-5.2
	2	x, y, z	11.52	B3LYP/6-31G(d,p)	-2.6	-0.4	-7.9	5.0	-6.9
	2	-x+1/2, -y, z+1/2	7.51	B3LYP/6-31G(d,p)	-5.3	-0.9	-20.3	13.2	-15.8
	2	x+1/2, -y+1/2, -z	5.11	B3LYP/6-31G(d,p)	-6.2	-1.7	-38.2	18.6	-29.7
	2	x+1/2, -y+1/2, -z	10.18	B3LYP/6-31G(d,p)	-2.1	-0.4	-7.5	5.4	-5.7

Scale factors for benchmarked energy models
See Mackenzie et al. IUCrJ (2017)

Energy Model	k_ele	k_pol	k_disp	k_rep
CE-HF ... HF/3-21G electron densities	1.019	0.651	0.901	0.811
CE-B3LYP ... B3LYP/6-31G(d,p) electron densities	1.057	0.740	0.871	0.618

Information

Crystal | Atoms | Surface | Energies

33′FBZP

Interaction Energies (kJ/mol)
R is the distance between molecular centroids (mean atomic position) in Å.

Total energies, only reported for two benchmarked energy models, are the sum of the four energy components, scaled appropriately (see the scale factor table below)

	N	Symop	R	Electron Density	E_ele	E_pol	E_dis	E_rep	E_tot
	2	x, y, z	6.14	B3LYP/6-31G(d,p)	-10.9	-2.8	-22.2	16.8	-22.5
	2	-x, -y, -z	5.44	B3LYP/6-31G(d,p)	-5.6	-1.8	-35.1	24.5	-22.7
	4	x+1/2, y+1/2, z	11.91	B3LYP/6-31G(d,p)	-1.6	-0.4	-5.0	3.8	-4.1
	2	-x, -y, -z	4.12	B3LYP/6-31G(d,p)	-10.8	-1.5	-47.9	27.0	-37.6
	2	-x+1/2, -y+1/2, -z	11.50	B3LYP/6-31G(d,p)	-4.5	-0.5	-8.0	4.3	-9.4

Scale factors for benchmarked energy models
See Mackenzie et al. IUCrJ (2017)

Energy Model	k_ele	k_pol	k_disp	k_rep
CE-HF ... HF/3-21G electron densities	1.019	0.651	0.901	0.811
CE-B3LYP ... B3LYP/6-31G(d,p) electron densities	1.057	0.740	0.871	0.618

Information

4FBZP

Crystal | Atoms | Surface | Energies

Interaction Energies (kJ/mol)
R is the distance between molecular centroids (mean atomic position) in Å.

Total energies, only reported for two benchmarked energy models, are the sum of the four energy components, scaled appropriately (see the scale factor table below)

	N	Symop	R	Electron Density	E_ele	E_pol	E_dis	E_rep	E_tot
	2	x, y, z	6.09	B3LYP/6-31G(d,p)	-9.9	-3.8	-21.5	16.0	-22.2
	2	x+1/2, -y+1/2, z+1/2	4.81	B3LYP/6-31G(d,p)	-5.6	-1.8	-39.7	25.4	-26.2
	2	x+1/2, -y+1/2, z+1/2	4.83	B3LYP/6-31G(d,p)	-4.7	-1.5	-39.5	24.5	-25.4
	2	-x+1/2, y+1/2, -z+1/2	11.44	B3LYP/6-31G(d,p)	-0.8	-0.1	-5.5	2.2	-4.4
	1	-x, -y, -z	11.87	B3LYP/6-31G(d,p)	-1.7	-0.3	-7.0	2.8	-6.3
	1	-x, -y, -z	12.64	B3LYP/6-31G(d,p)	0.8	-0.2	-3.1	0.0	-2.0
	1	-x, -y, -z	10.34	B3LYP/6-31G(d,p)	-3.7	-0.5	-11.6	11.1	-7.6
	1	-x, -y, -z	11.23	B3LYP/6-31G(d,p)	-0.4	-0.2	-4.5	10.1	1.8

Scale factors for benchmarked energy models
See Mackenzie et al. IUCrJ (2017)

Energy Model	k_ele	k_pol	k_disp	k_rep
CE-HF ... HF/3-21G electron densities	1.019	0.651	0.901	0.811
CE-B3LYP ... B3LYP/6-31G(d,p) electron densities	1.057	0.740	0.871	0.618

Information

4MBZP_I Grey

Crystal | Atoms | Surface | Energies

Interaction Energies (kJ/mol)
R is the distance between molecular centroids (mean atomic position) in Å.

Total energies, only reported for two benchmarked energy models, are the sum of the four energy components, scaled appropriately (see the scale factor table below)

	N	Symop	R	Electron Density	E_ele	E_pol	E_dis	E_rep	E_tot
	1	-	4.66	B3LYP/6-31G(d,p)	-3.9	-2.6	-49.2	32.5	-28.9
	1	-x, -y, -z	9.49	B3LYP/6-31G(d,p)	-10.8	-3.3	-16.2	14.3	-19.2
	1	-	4.84	B3LYP/6-31G(d,p)	-3.5	-1.2	-37.9	23.0	-23.4
	1	-x, -y, -z	7.49	B3LYP/6-31G(d,p)	-20.9	-5.2	-22.2	22.0	-31.7
	1	-x, -y, -z	12.15	B3LYP/6-31G(d,p)	-0.8	-0.2	-7.1	0.0	-7.2
	1	-	8.89	B3LYP/6-31G(d,p)	-3.9	-1.2	-18.8	10.1	-15.2
	1	-	11.77	B3LYP/6-31G(d,p)	-1.2	-0.2	-7.7	3.3	-6.1
	2	x, y, z	13.87	B3LYP/6-31G(d,p)	0.9	-0.5	-4.9	0.0	-3.7
	1	-x, -y, -z	6.42	B3LYP/6-31G(d,p)	-5.5	-1.0	-27.2	17.8	-19.2
	1	-	5.50	B3LYP/6-31G(d,p)	-7.2	-1.6	-42.7	28.0	-28.7
	1	-	7.26	B3LYP/6-31G(d,p)	-14.1	-2.8	-35.0	28.1	-30.1
	1	-	8.60	B3LYP/6-31G(d,p)	-2.4	-0.8	-3.0	0.4	-5.5

Scale factors for benchmarked energy models
See Mackenzie et al. IUCrJ (2017)

Energy Model	k_ele	k_pol	k_disp	k_rep
CE-HF ... HF/3-21G electron densities	1.019	0.651	0.901	0.811
CE-B3LYP ... B3LYP/6-31G(d,p) electron densities	1.057	0.740	0.871	0.618

Information

4MBZP_I Magenta

Crystal | Atoms | Surface | Energies

Interaction Energies (kJ/mol)
R is the distance between molecular centroids (mean atomic position) in Å.

Total energies, only reported for two benchmarked energy models, are the sum of the four energy components, scaled appropriately (see the scale factor table below)

	N	Symop	R	Electron Density	E_ele	E_pol	E_dis	E_rep	E_tot
	1	-	4.66	B3LYP/6-31G(d,p)	-3.9	-2.6	-49.2	32.5	-28.9
	0	-x, -y, -z	9.49	B3LYP/6-31G(d,p)	-10.8	-3.3	-16.2	14.3	-19.2
	1	-	4.84	B3LYP/6-31G(d,p)	-3.5	-1.2	-37.9	23.0	-23.4
	0	-x, -y, -z	7.49	B3LYP/6-31G(d,p)	-20.9	-5.2	-22.2	22.0	-31.7
	0	-x, -y, -z	12.15	B3LYP/6-31G(d,p)	-0.8	-0.2	-7.1	0.0	-7.2
	1	-	8.89	B3LYP/6-31G(d,p)	-3.9	-1.2	-18.8	10.1	-15.2
	1	-	11.77	B3LYP/6-31G(d,p)	-1.2	-0.2	-7.7	3.3	-6.1
	0	x, y, z	13.87	B3LYP/6-31G(d,p)	0.9	-0.5	-4.9	0.0	-3.7
	0	-x, -y, -z	6.42	B3LYP/6-31G(d,p)	-5.5	-1.0	-27.2	17.8	-19.2
	1	-	5.50	B3LYP/6-31G(d,p)	-7.2	-1.6	-42.7	28.0	-28.7
	1	-	7.26	B3LYP/6-31G(d,p)	-14.1	-2.8	-35.0	28.1	-30.1
	1	-	8.60	B3LYP/6-31G(d,p)	-2.4	-0.8	-3.0	0.4	-5.5
	1	-x, -y, -z	9.43	B3LYP/6-31G(d,p)	-8.5	-3.0	-14.2	10.7	-17.0
	2	x, y, z	13.87	B3LYP/6-31G(d,p)	1.3	-0.5	-5.1	0.0	-3.5
	1	-x, -y, -z	7.78	B3LYP/6-31G(d,p)	-18.8	-4.7	-19.6	14.9	-31.2
	1	-x, -y, -z	6.32	B3LYP/6-31G(d,p)	-7.4	-1.2	-30.5	20.2	-22.8
	1	-x, -y, -z	11.87	B3LYP/6-31G(d,p)	-1.6	-0.3	-8.9	6.6	-5.5

Scale factors for benchmarked energy models
See Mackenzie et al. IUCrJ (2017)

Energy Model	k_ele	k_pol	k_disp	k_rep
CE-HF ... HF/3-21G electron densities	1.019	0.651	0.901	0.811
CE-B3LYP ... B3LYP/6-31G(d,p) electron densities	1.057	0.740	0.871	0.618

Information

4MBZP_II

Crystal | Atoms | Surface | Energies

Interaction Energies (kJ/mol)
R is the distance between molecular centroids (mean atomic position) in Å.

Total energies, only reported for two benchmarked energy models, are the sum of the four energy components, scaled appropriately (see the scale factor table below)

	N	Symop	R	Electron Density	E_ele	E_pol	E_dis	E_rep	E_tot
	2	x, y, z	6.14	B3LYP/6-31G(d,p)	-8.4	-4.3	-23.9	15.9	-23.0
	2	x, -y, z+1/2	4.87	B3LYP/6-31G(d,p)	-6.7	-2.0	-43.0	28.5	-28.4
	2	x+1/2, y+1/2, z	12.53	B3LYP/6-31G(d,p)	-0.6	-0.1	-2.6	0.0	-2.9
	2	x+1/2, y+1/2, z	12.53	B3LYP/6-31G(d,p)	1.7	-0.3	-4.4	0.0	-2.3
	2	x, -y, z+1/2	4.73	B3LYP/6-31G(d,p)	-5.3	-3.1	-49.4	33.1	-30.4
	2	x+1/2, -y+1/2, z+1/2	11.89	B3LYP/6-31G(d,p)	-4.6	-0.9	-8.8	10.6	-6.7
	2	x+1/2, -y+1/2, z+1/2	12.82	B3LYP/6-31G(d,p)	-1.7	-0.5	-6.6	0.0	-7.8

Scale factors for benchmarked energy models
See Mackenzie et al. IUCrJ (2017)

Energy Model	k_ele	k_pol	k_disp	k_rep
CE-HF ... HF/3-21G electron densities	1.019	0.651	0.901	0.811
CE-B3LYP ... B3LYP/6-31G(d,p) electron densities	1.057	0.740	0.871	0.618

Table S5. Topological parameters for the interactions obtained from QTAIM calculations in substituted benzophenones. (Motifs are considered in accordance with *PIXEL* method)

Compound	Motif	Interaction	R*ij* (Å)	ρ (e/Å^3)	$\nabla^2\rho$ (e/Å^5)	V (au)	G (au)	$\|V\|$/G
2F4′FBZP	**I**	H10···O1	2.547	0.04	0.55	-0.0039	0.0048	0.82
		H10···C13	2.665	0.04	0.49	-0.0027	0.0039	0.69
	II	H5···F1	2.368	0.04	0.74	-0.0049	0.0063	0.79
	III	H12···O1	2.579	0.04	0.50	-0.0032	0.0042	0.76
		H7···H13	2.372	0.03	0.40	-0.0018	0.0029	0.62
	IV & V	H5···F2	2.459	0.04	0.68	-0.0043	0.0057	0.75
		H12···F2	2.509	0.04	0.78	-0.0047	0.0064	0.73
3F3′FBZP	**I**	H7···O1	2.580	0.04	0.59	-0.0037	0.0049	0.75
	II	H7···H7	2.214	0.03	0.48	-0.0025	0.0037	0.67
	III	H5···F1(Dimer)	2.642	0.03	0.49	-0.0025	0.0038	0.66
	IV	H5···F1	2.456	0.03	0.62	-0.0040	0.0052	0.76
4FBZP	**I**	H7···O1	2.587	0.04	0.62	-0.0039	0.0052	0.75
		H13···O1	2.609	0.04	0.59	-0.0036	0.0049	0.75
	II & III	H6···C13	2.853	0.03	0.39	-0.0023	0.0032	0.73
		H3···C10	3.159	0.03	0.32	-0.0019	0.0026	0.73
		H9···C4	2.800	0.03	0.41	-0.0024	0.0033	0.72
		H12···C6	3.143	0.03	0.32	-0.0019	0.0026	0.74
	IV	H4···F1	2.468	0.04	0.64	-0.0040	0.0053	0.75
	V	H10···F1A	2.809	0.02	0.41	-0.0019	0.0031	0.64
	VI	H10···F1	2.669	0.03	0.48	-0.0025	0.0037	0.67
	VII	F1···F1	2.778	0.12	2.04	-0.0188	0.0199	0.94
	VIII	F1A···F1A	2.137	0.17	3.27	-0.0272	0.0306	0.89
4MBZP_I	**I & IV**	H28A···O3	2.548	0.04	0.54	-0.0037	0.0046	0.79
		H3···O4	2.629	0.04	0.53	-0.0035	0.0045	0.77
		H4···C20	2.765	0.04	0.45	-0.0027	0.0037	0.74
		H14A···O3	2.539	0.05	0.62	-0.0044	0.0054	0.82
		H14···C16	2.734	0.04	0.44	-0.0026	0.0036	0.73
	II	H14B···O1	2.407	0.05	0.68	-0.0053	0.0062	0.86
	III & V	H27···O2	2.877	0.04	0.57	-0.0035	0.0047	0.75
		H6···C17	2.720	0.04	0.44	-0.0027	0.0036	0.73
		H20···C6	3.030	0.04	0.44	-0.0027	0.0036	0.74
	VI	H10···O1	2.644	0.03	0.47	-0.0029	0.0039	0.75
	VII	H24···O3	2.668	0.03	0.45	-0.0028	0.0037	0.74
4MBZP_II	**I**	H14C···C5	2.780	0.03	0.42	-0.0023	0.0033	0.68
	II	H3···C4	2.756	0.04	0.45	-0.0027	0.0037	0.73
	III	H13···O1	2.702	0.03	0.49	-0.0029	0.0041	0.73
		H7···O1	2.669	0.04	0.54	-0.0032	0.0044	0.73
	IV	H11···O2	2.357	0.06	0.76	-0.0067	0.0073	0.91

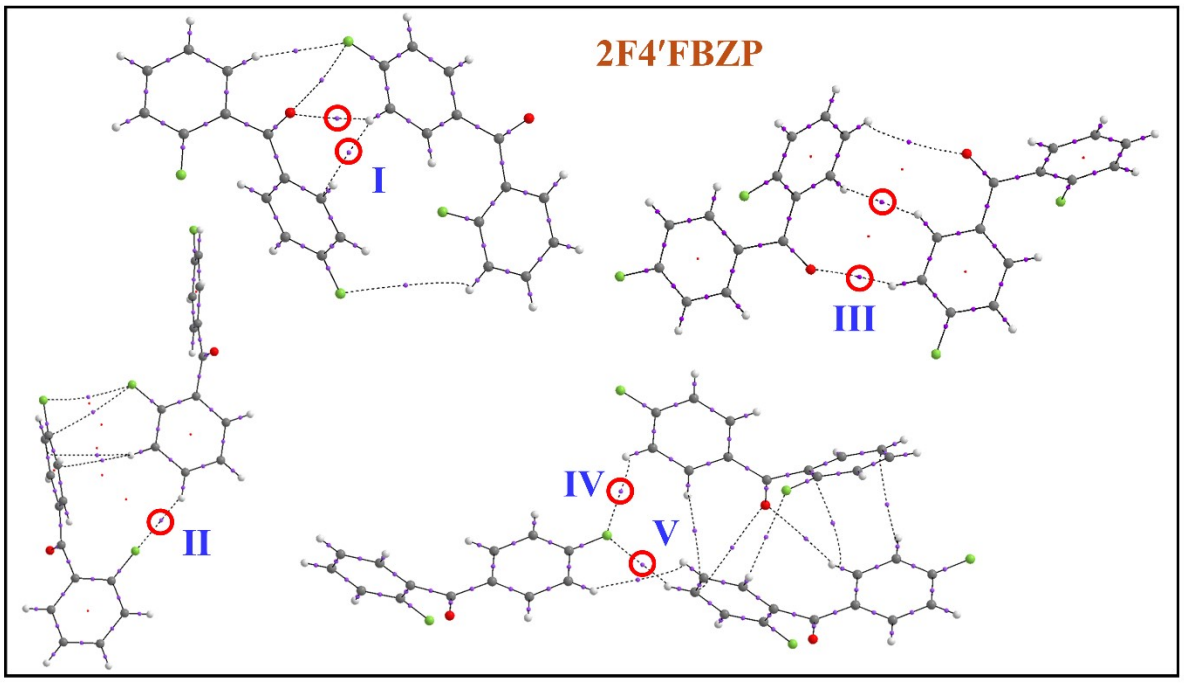
2F4′FBZP
I
II
III
IV
V

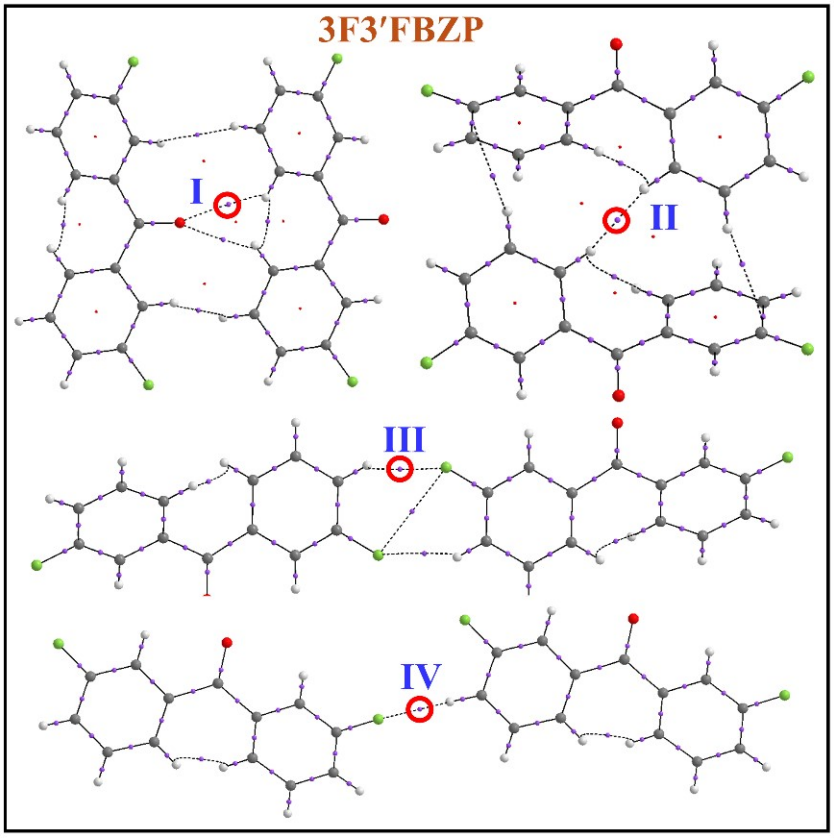
3F3′FBZP
I
II
III
IV

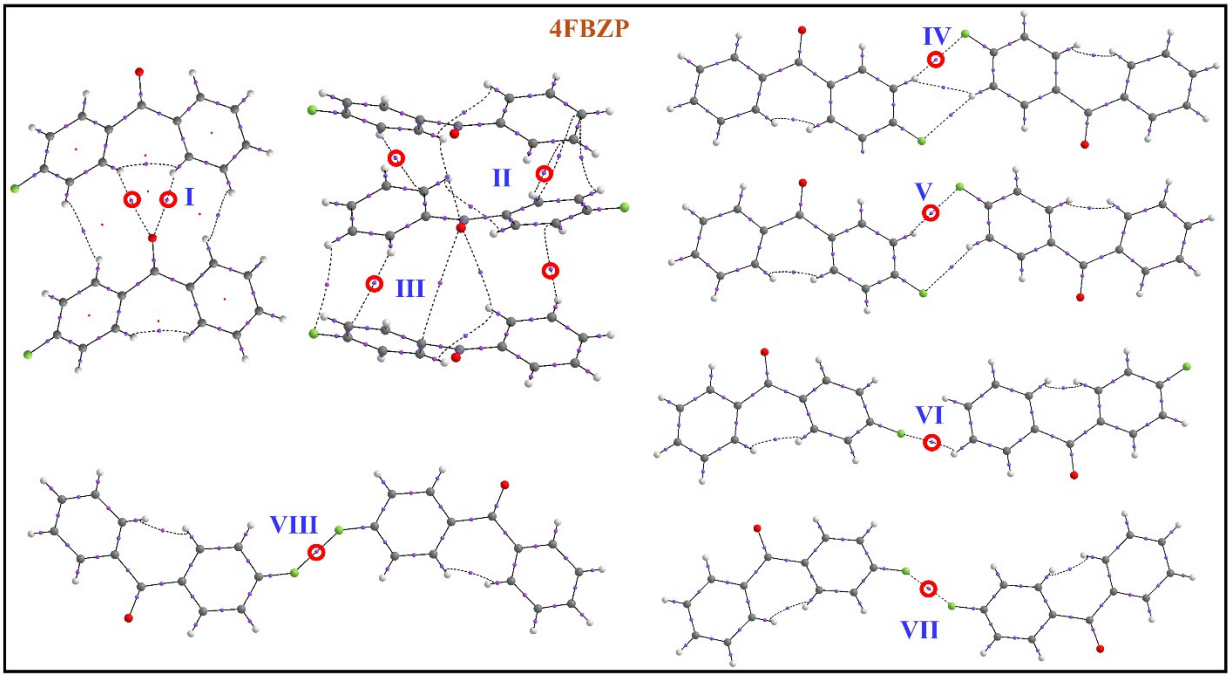
4FBZP
I
II
III
IV
V
VI
VII
VIII

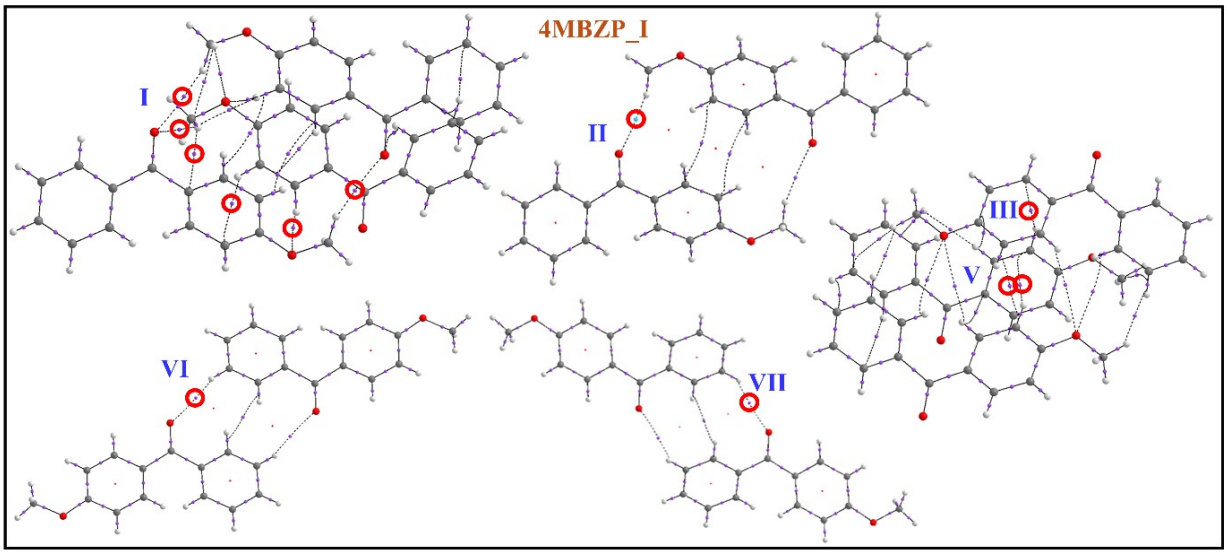
4MBZP_I
I
II
III
V
VI
VII

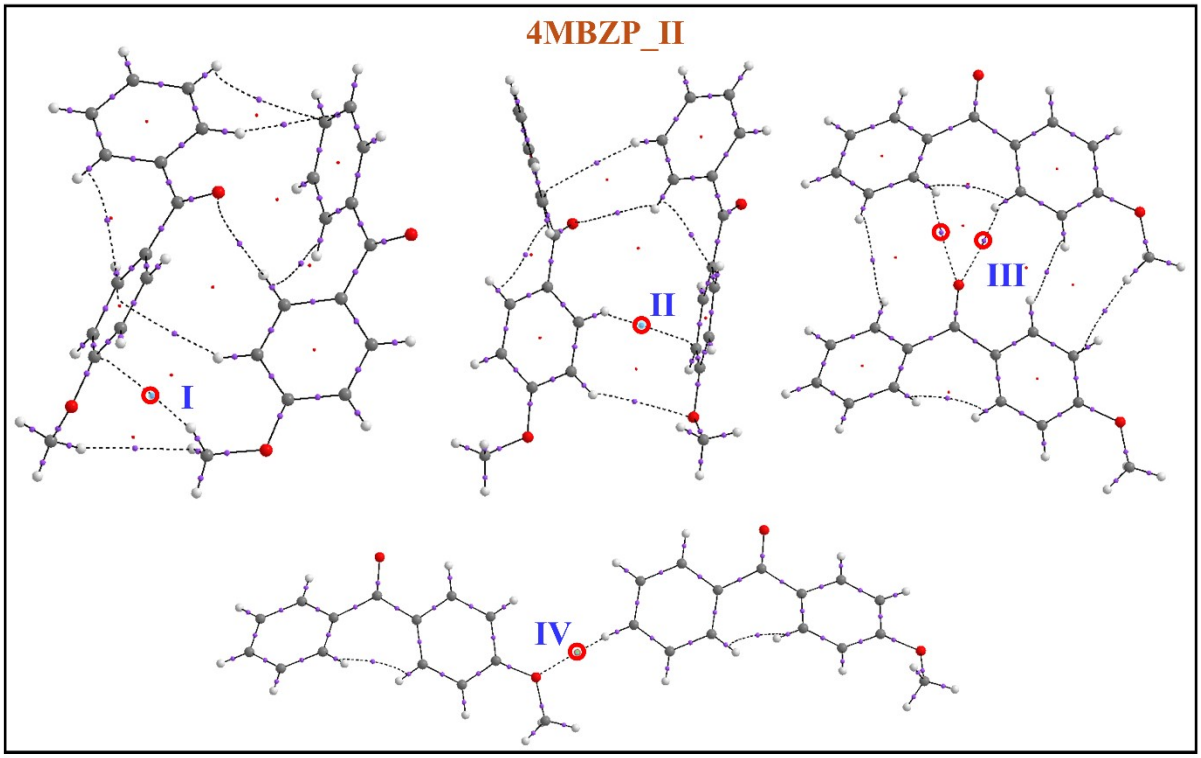

Fig. S5 Depiction of bond critical points (highlighted in red circles) and the associated bond paths, connecting the atoms in individual motifs of all substituted benzophenones.

Table S6. Quantum Efficiency results

Sample	Quantum efficiency (%)
2F4′FBZP	**<1**
3F3′FBZP	**0.3**
4FBZP	**9.5**
4MBZP_I	**<1**

- **Calculation part of τ_{avg}**

$\langle\tau_{avg}\rangle = (\tau_1A_1 + \tau_2A_2 + \tau_3A_3)/100$

$= (0.269\times58) + (0.900\times36) + (0.857\times6) =$ **1.0 ms**

Where, A1+A2+A3=100% i.e, 58+36+6= 100%

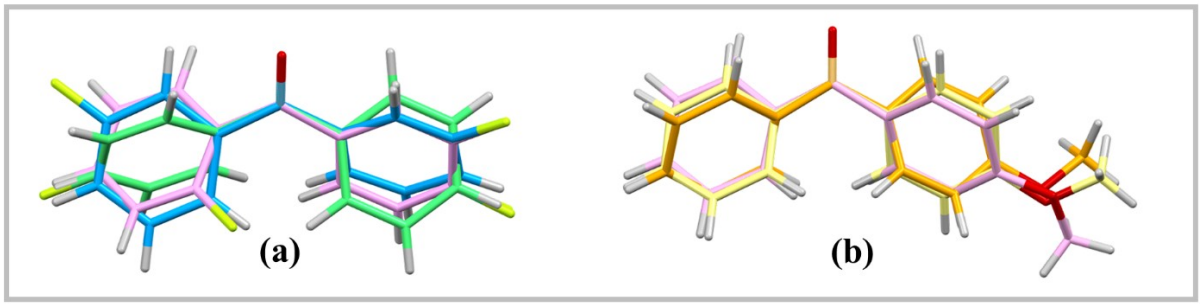

Fig. S6 Structural overlay of (a) 2F4′FBZP (Pink), 3F3′FBZP (Blue), and 4FBZP (Green); and (b) polymorph: 4MBZP_I (Yellow (1) and Orange (2)) and 4MBZP_II (Pink).

Table S7. The static structural details of 2F4′FBZP, 3F3′FBZP, 4FBZP and 4MBZP_I.

Compound	a(Å)	b(Å)	c(Å)	α	β	γ	Energy(au)	Energy/atom (au)
2F4′FBZP	8.39	9.19	11.59	90	90	90	-570.85	-5.95
3F3′FBZP	11.51	3.07	14.11	80.56	99.44	150.14	-570.88	-5.95
4FBZP	6.15	21.13	7.19	90	90	90	-570.86	-5.95
4MBZP_I	9.17	8.94	13.09	87.92	71.2	70.5	-473.52	-4.23

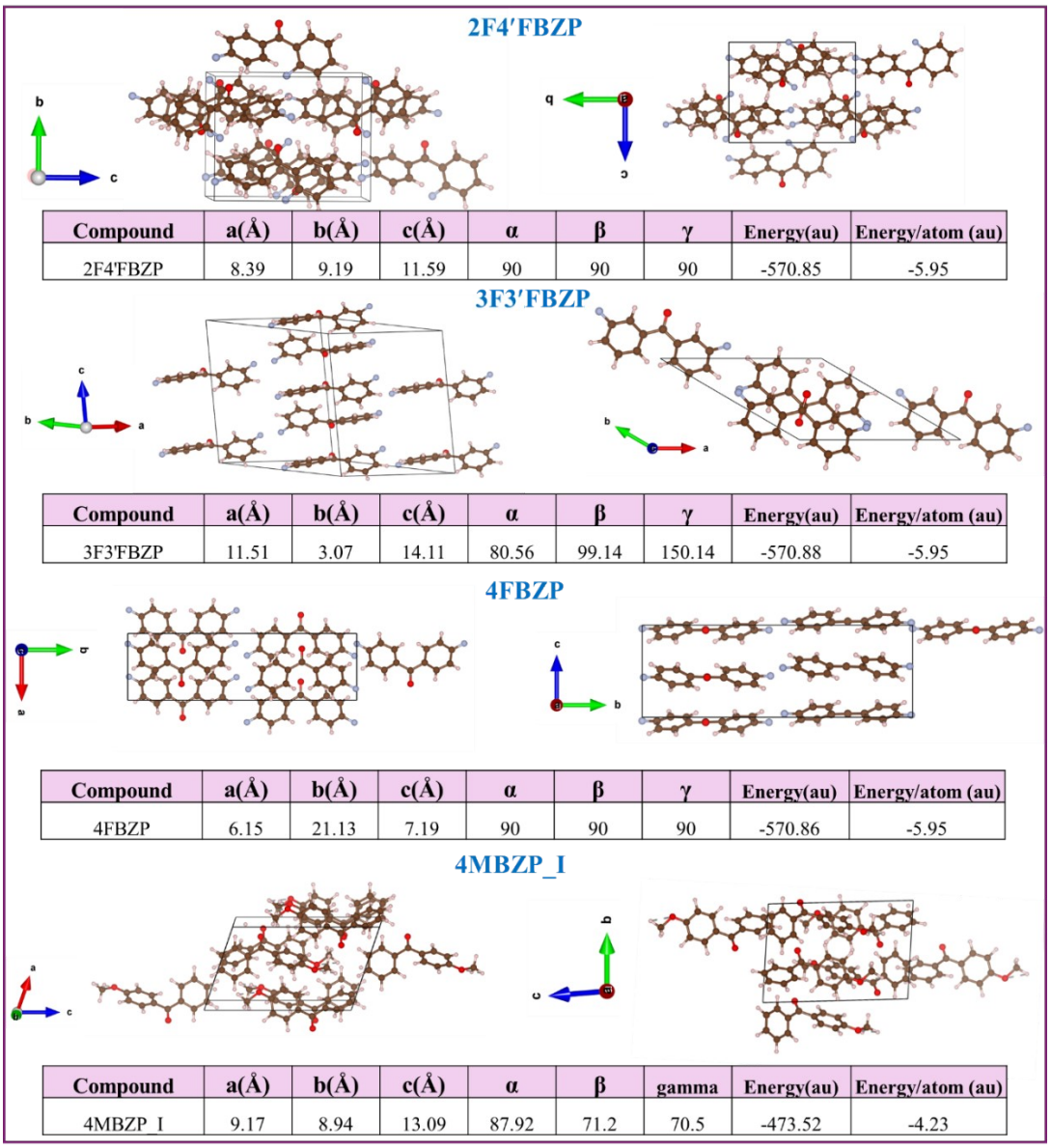

Compound	a(Å)	b(Å)	c(Å)	α	β	γ	Energy(au)	Energy/atom (au)
2F4'FBZP	8.39	9.19	11.59	90	90	90	-570.85	-5.95

Compound	a(Å)	b(Å)	c(Å)	α	β	γ	Energy(au)	Energy/atom (au)
3F3'FBZP	11.51	3.07	14.11	80.56	99.14	150.14	-570.88	-5.95

Compound	a(Å)	b(Å)	c(Å)	α	β	γ	Energy(au)	Energy/atom (au)
4FBZP	6.15	21.13	7.19	90	90	90	-570.86	-5.95

Compound	a(Å)	b(Å)	c(Å)	α	β	gamma	Energy(au)	Energy/atom (au)
4MBZP_I	9.17	8.94	13.09	87.92	71.2	70.5	-473.52	-4.23

Fig. S7 The DFT optimized geometries and static structural details of 2F4′FBZP, 3F3′FBZP, 4FBZP, and 4MBZP.

References

1) SADABS, version 2014/5; Bruker AXZ Inc., Madison, Wisconsin, USA, **2014**.
2) G. M. Sheldrick, *Acta Crystallogr. Sect. C Struct. Chem.*, 2015, **71**, 3–8.
3) M. Nardelli, *J.Appl. Cryst.*, 1995, **28**, 659.
4) C. F. MacRae, I. Sovago, S. J. Cottrell, P. T. A. Galek, P. McCabe, E. Pidcock, M. Platings, G. P. Shields, J. S. Stevens, M. Towler and P. A. Wood, *J. Appl. Crystallogr.*, 2020, **53**, 226–235.
5) D. Giron, *Thermochim. Acta*, 1995, **248**, 1–59.
6) M. J. Frisch, G.W. Trucks, H.B.Schlegel, et al. *Gaussian09: revision D.1*; Gaussian, Inc.,Wallingford CT, 2016.

7) P. R. Spackman, M. J. Turner, J. J. McKinnon, S. K. Wolff, D. J. Grimwood, D. Jayatilaka and M. A. Spackman, *J. Appl. Crystallogr.*, 2021, **54**, 1006–1011.
8) M. A. Spackman and J. J. McKinnon, *CrystEngComm*, 2002, **4**, 378–392.
9) J. J. McKinnon, M. A. Spackman and A. S. Mitchell, *Acta Crystallogr. Sect. B Struct. Sci.,* 2004, **B60**, 627-668.
10) C. F. Mackenzie, P. R. Spackman, D. Jayatilaka and M. A. Spackman, *IUCrJ*, 2017, **4**, 575–587.
11) A. Gavezzotti, *New J. Chem.*, 2011, **35**, 1360–1368.
12) L. Maschio, B. Civalleri, P. Ugliengo and A. Gavezzotti, *J. Phys. Chem. A*, 2011, **115**, 11179–11186.
13) A. Gavezzotti, *J. Phys. Chem. B*, 2003, **107**, 2344–2353.
14) R. F. W. Bader, *Acc. Chem. Res.*, 1985, **18**, 9–15.
15) T.A. Keith, *AIMAll (VERsion 19.10.12) TK Gristmill Software*, Overland Park KS,USA, 2019.
16) W. Kohn, A. D. Becke and R. G. Parr, *J. Phys. Chem.*, 1996, **100**, 12974–12980.
17) S. Goedecker and M. Teter, *Phys. Rev. B - Condens. Matter Mater. Phys.*, 1996, **54**, 1703–1710.
18) J.P. Perdew, K. Bruke, M.Ernzerhof, *Phys. Rev. Letters.* 1996, **77(18)**, 3865-3868.
19) T. M. Henderson, B. G. Janesko and G. E. Scuseria, *J. Phys. Chem. A*, 2008, **112**, 12530–12542.
20) M. Guidon, J. Hutter and J. Vandevondele, *J. Chem. Theory Comput.*, 2010, **6**, 2348–2364.
21) E. Hamzehpoor and D. F. Perepichka, *Angew. Chemi. Int. Ed.,* 2020, **59**, 9977-9981.
22) M.J. Frisch, G. W. Trucks, H. B. Schlegel, G. E. Scuseria, M. A. Robb, J. R. Cheeseman, J. A. Montgomery, et al. Gaussian 09; Gaussian, Inc.: Wallingford, CT, 2009.
23) T. D. Kühne, M. Iannuzzi, M. Del Ben, V. V. Rybkin, P. Seewald, F. Stein, T. Laino, R. Z. Khaliullin, O. Schütt, F. Schiffmann, D. Golze, J. Wilhelm, S. Chulkov, M. H. Bani-Hashemian, V. Weber, U. Borštnik, M. Taillefumier, A. S. Jakobovits, A. Lazzaro, H. Pabst, T. Müller, R. Schade, M. Guidon, S. Andermatt, N. Holmberg, G. K. Schenter, A. Hehn, A. Bussy, F. Belleflamme, G. Tabacchi, A. Glöß, M. Lass, I. Bethune, C. J. Mundy, C. Plessl, M. Watkins, J. VandeVondele, M. Krack and J. Hutter, *J. Chem. Phys.*, **2020**, *152* (19), 1-47.
24) H. Solařová, I. Císařová and P. Štěpnička, *Organometallics*, 2014, **33**, 4131–4147.
25) G. Shouwu, S. Genbo, P. Feng, H. Youping, *Acta Cryst.*1992, **C48**, 576–578.